A&A 420, 673–681 (2004)
DOI: 10.1051/0004-6361:20035651

Astronomy & Astrophysics

Chemical composition of the magnetic B star HR 5049⋆,⋆⋆

M. Nishimura[1], K. Sadakane[2], K. Kato[3], Y. Takeda[4], and G. Mathys[5]

[1] Rakutou High School, Anshu, Yamashina-ku, Kyoto 607-8017, Japan
[2] Astronomical Institute, Osaka Kyoiku University, Asahigaoka, Kashiwara, Osaka 582-8582, Japan
[3] Osaka Science Museum, Nakanoshima, Kita-ku, Osaka 530-0005, Japan
[4] National Astronomical Observatory, Osawa, Mitaka, Tokyo 181-8588, Japan
[5] European Southern Observatory, Casilla 19001, Santiago 19, Chile

Received 10 November 2003 / Accepted 23 February 2004

Abstract. A spectrum synthesis analysis for photospheric lines in the magnetic B star HR 5049 is presented, based on a high quality spectrogram obtained with the EMMI spectrograph attached to the NTT at ESO. It is found that light elements such as He, C and O are under-abundant. One of the most notable features is the deficiency of He by more than −2.0 dex. Co and Cl are over-abundant by +3.5 dex and +1.9 dex, respectively. Other iron peak elements are over-abundant ranging from +0.47 dex (Ti II) to +1.94 dex (Cr I). For rare earth elements, the lines of once-ionized species are generally weak, while the third spectra (especially those of Pr and Nd) are very prominent. Although rare earth elements show significant over-abundances ranging from +3.0 dex to as large as +4.0 dex, Ba has the solar abundance. The Nd-Pr abundance difference, which shows an apparent decreasing trend with increasing effective temperature among CP stars, is found to be unusually small in HR 5049.

Key words. stars: abundances – stars: chemically peculiar – stars: individual: HR 5049

1. Introduction

Among the upper main sequence stars on the HR diagram there exist a large number of chemically peculiar (CP) stars. In these stars, the magnetic A and B type chemically peculiar (CP2) stars show a variety in their chemical composition. These chemical peculiarities are known to be associated with strong magnetic fields. A few stars including HR 5049 (HD 116 458) exhibit extraordinary strong Co I and Co II lines. In addition, Cl II lines are also detected in these stars. HR 1094 (HD 22 316) is a typical star with this Cl–Co peculiarity. The Co anomaly of HR 1094 was first noted by Cowley & Aikman (1980). Sadakane (1992) and Nielsen & Wahlgren (2000) analyzed the optical region spectra of HR 1094 to demonstrate the striking anomalies (over-abundances) of Cl and Co.

A southern sixth magnitude B-type star HR 5049, a single-lined spectroscopic binary with a period of 126.18 d (Dworetsky 1982), is another well-known star with a Co peculiarity. It was first pointed out by Dworetsky et al. (1980), who identified strong Co I and Co II lines and estimated the abundance to be in excess by +3.0 dex using the curve of growth technique. Resolved Zeeman split lines were observed by Mathys et al. (1997), from which they derived a mean magnetic field modulus of 4.7 kG. Mathys & Hubrig (1997) found that the mean longitudinal magnetic field of HR 5049 is around −2 kG. Recently, a magnetic field geometry of HR 5049 was modeled by Landstreet & Mathys (2000). Hensberge (1993) determined its photometric period to be 147.9 ± 0.6 d. He showed that the period reproduces the regular variation of the magnetic field.

Dworetsky et al. (1980) suggested that the rotational velocity of HR 5049 is less than 6 km s^{-1}, while Nielsen & Wahlgren (2000) obtained $v \sin i$ = 4 km s^{-1} from a profile analysis of the Fe II λ 4508 Å line.

Nishimura (1998) (hereafter Paper I) performed a detailed LTE abundance analysis of HR 5049 using the spectra between λ 5700 Å and λ 6700 Å. He used five spectrograms obtained with CASPEC attached to the 3.6 m reflector at the European Southern Observatory, La Silla. These spectra had been taken for spectropolarimetric study by Mathys. Nishimura (1998) found over-abundances of Cl (+3.3 dex, upper limit), Co (+4.0 dex), Si (+1.3 dex), Cr (+2.8 dex), and Fe (+1.6 dex). Line intensities of Pr III were shown to vary with the rotation period (147.9 d). The abundance pattern in HR 5049 is similar to that of HR 1094.

Since the spectral coverage of the data used in Paper I was limited to the red spectral region, the analysis was performed for only a few elements. In this study, we have analyzed a

Send offprint requests to: M. Nishimura,
e-mail: mnisimura@kcat.zaq.ne.jp

⋆ Based on observations collected at the La Silla Observatory, ESO (Chile) with the New Technology Telescope (NTT).

⋆⋆ The full Table 2 is only available in electronic form at the CDS via anonymous ftp to cdsarc.u-strasbg.fr (130.79.128.5) or via
http://cdsweb.u-strasbg.fr/cgi-bin/qcat?J/A+A/420/673

Table 1. Ionization equilibria between Fe I and Fe II, and between Co I and Co II. Each abundance was given for two model atmospheres.

	(10 300, 3.81)	(11 000, 4.00)
Fe I	8.32 ± 0.17	8.64 ± 0.18
Fe II	8.29 ± 0.32	8.43 ± 0.28
Co I	8.43 ± 0.08	8.72 ± 0.10
Co II	8.35 ± 0.37	8.38 ± 0.34

higher resolution spectrum of HR 5049 covering both blue and red spectral regions. We adopted the spectrum synthesis technique to explicitly include the effect of magnetic intensification. Special attention has been paid to quantitative evaluations of abundance anomalies for both light and heavy (rare earth) elements.

2. Observational data

We use a CCD spectrogram ranging from λ 4070 Å to λ 6700 Å which was obtained with the ESO New Technology Telescope (NTT) and the ESO Multi-Mode Instrument (EMMI) in the cross-dispersed echelle mode. The achieved resolving power is on average 70 000, with variations of a few percent through the observed range. The time of mid-exposure for this observation was HJD 2 450 115.790. The achieved S/N ratio is estimated to range from 100 to 150. The detailed process of data reduction is described in Mathys & Hubrig (2004).

The candidate lines in the wavelength region between λ 4070 Å and λ 6700 Å were taken from the Kurucz CD-ROM (Kurucz & Bell 1995) and VALD atomic line database (Kupka et al. 1999) using a spectrum synthesis technique. Telluric lines were carefully removed by consulting the table of the solar spectral lines (Moore et al. 1966).

To identify the lines of heavy elements usually not detected in normal stars, we calculated both equivalent widths and synthetic spectra assuming 10^4 times the solar abundance for the element in question. The lines of heavy elements strong enough to be analyzed were identified in this way. However, it should be noted that many strong lines still remain unidentified. This implies the incompleteness of presently-available atomic line data, especially those of the third spectra of heavy elements.

3. Model parameters and the spectrum synthesis

The atmospheric parameters ($T_{\rm eff}$ = 10 300 K, and $\log g$ = 3.81) are taken from Hubrig et al. (2000). The effective temperature is determined from the *uvby-β* photometric data applying the calibration of Moon and Dworetsky (1985) and Geneva photometric data. The surface gravity is obtained from the basic relation between stellar masses, radius and gravity using parallax data given in the HIPPARCOS catalog. In Paper I, we used $T_{\rm eff}$ = 11 000 K, $\log g$ = 4.0, and [M/H] = +1.0 determined from Geneva photometric data and from *uvby-β* photometric data applying the calibration formula with a ten times solar metal composition model. The former data were calibrated by North & Nicolet (1994), and the latter data were calibrated by Lester et al. (1986).

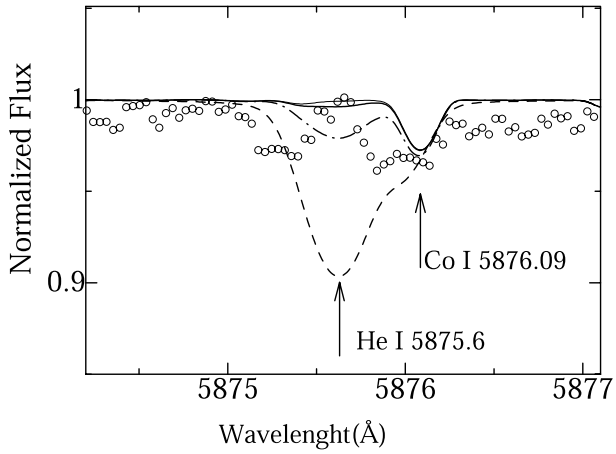

Fig. 1. The synthetic spectrum around the He I line at λ 5875.6 Å. Computations were carried out using a model atmosphere with $T_{\rm eff}$ = 10 300 K. Open circles – the observed spectrum, dashed line – solar abundance, dot-dashed line – −1.0 dex, solid line – −2.0 dex (adopted), and thin solid line – −3.0 dex compared with the solar value.

After examining the ionization equilibria between Fe I and Fe II, and between Co I and Co II as shown in Table 1, we decided to choose a cooler ($T_{\rm eff}$ = 10 300 K, and $\log g$ = 3.81) model atmosphere instead of the model used in paper I ($T_{\rm eff}$ = 11 000 K, and $\log g$ = 4.00). Recently, Adelman et al. (2000) obtained $T_{\rm eff}$ = 11 300 K and log$g$ = 3.95 for HR 5049 from *uvby-β* photometry, and Nielsen & Wahlgren (2000) obtained $T_{\rm eff}$ = 10 500 K and $\log g$ = 4.0 for HR 5049. The atmospheric parameters adopted in this study are closer to those of Nielsen & Wahlgren (2000).

We find no He I line in the spectrum. In Fig. 1, we compare the observed profile with the computed ones of the He I λ 5875.6 Å line. This figure suggests that He is extremely under-abundant: an upper limit of −2.0 dex with respect to the solar value is obtained. The considerable He deficiency may affect the atmospheric structure and hence may introduce errors in the abundance determinations. To examine this point, we constructed a model atmosphere with the program ATLAS9 (Kurucz 1993) having the above low He content. The elemental abundance computed with the low He-content model atmosphere is found to change only slightly (within 0.04 dex) compared with the case of a model atmosphere of normal He content.

Castelli & Kurucz (1994) and Castelli et al. (1997) analyzed Vega and the ^{3}He star 3 Cen A (HD 120 709), respectively, using opacity sampling ATLAS12 (Kurucz 1996) model atmospheres. In the case of 3 Cen A, Castelli et al. (1997) constructed both ATLAS9 and ATLAS12 model atmospheres with the same atmospheric parameters, and compared the T–log ($\tau_{\rm Ross}$) relations and the flux distributions. They found a slight change in the T–log ($\tau_{\rm Ross}$) relation only in the layers for log ($\tau_{\rm Ross}$) $\leq$ −3.5 and nearly the same computed energy distributions. They found no significant difference between ATLAS9 and ATLAS12 model atmospheres. We guess that the effect of the low He content on the resulting abundances will be small for HR 5049.

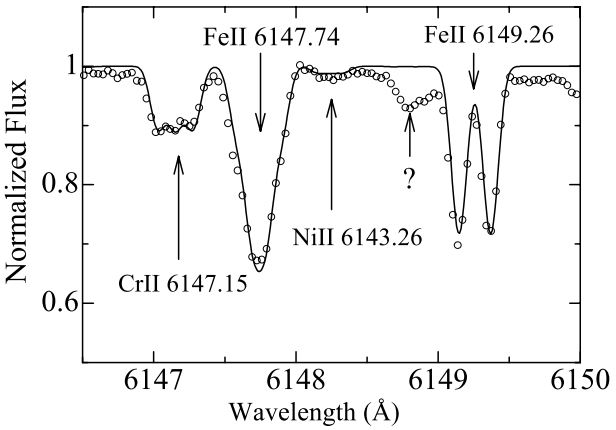

Fig. 2. The synthetic spectrum around the Fe II λ 6147 Å and λ 6149 Å lines. Open circles represent the observed spectrum, the solid line is for the adopted abundance (log ϵ (Fe II) = 8.54) with the 4.7 kG magnetic field, ξ_t = 0 km s^{-1}. An unidentified feature is indicated by a question mark.

Since the resolved Zeeman split lines due to the magnetic field of this star (4.7 kG) are observed by Mathys (1990), we took the effect of magnetic intensifications into account for the spectrum synthesis. The computation was made by the spectrum synthesis code SPSHOW developed by Takeda (2000). The magnetic field was incorporated in a simple manner, where the line opacity includes Zeeman components while neglecting any polarization effect (i.e., Case (c) in Sect. 2.1 of Takeda 1993). The strengths of the Zeeman components were computed by assuming the LS coupling, where the necessary quantum numbers (L, S, J) for the upper and lower levels were taken from the VALD database (Kupka et al. 1999) and NIST home page (2000). In Fig. 2, we show an example of our synthesized spectrum for the pair of Fe II λ 6147 Å and λ 6149 Å. Observed profiles of these two Fe II lines can be reproduced by incorporating the 4.7 kG magnetic field. We adopted this magnetic field in the final abundance computations. In the following magnetic spectrum synthesis, we assume the zero km s^{-1} microturbulence. An instrumental broadening corresponding to the resolving power of 70 000 was also applied.

We adopted $v \sin i$ = 4 ± 1 km s^{-1} as a projected rotational velocity, which was determined from a profile analysis of the Fe II λ 4508 Å line, in agreement with that obtained by Nielsen & Wahlgren (2000). Although the effective Landé factor of this line is *not* zero (0.500), it is clean and strong enough to be used in the determination of $v \sin i$. Another clean Fe II line at λ 4314.31 Å line, which has the effective Landé factor of 0.360, also shows $v \sin i$ = 4 ± 1 km s^{-1}. The two Fe I lines at λ 5434.52 Å and λ 5576.09 Å both have very small effective Landé factors (−0.01), are recommended in Kochukhov (2003) to be suitable for the determination of $v \sin i$. Unfortunately, however, these two lines are extremely weak and heavily blended in HR 5049.

When we take the photometric period of 147.9 d obtained by Hensberge (1993) and the radius of 3.54 ± 0.39 (in units of solar radius) obtained by Hubrig et al. (2000) into account, this $v \sin i$ = 4 km s^{-1} may be slightly large. We suppose that some other broadening mechanisms must contribute to the apparent $v \sin i$.

Table 2. Analyses of individual atomic lines. Columns from left to right are: the names of ion, wavelength in Å, excitation potential (χ) in eV, log gf value, reference for log gf, log ϵ, the remark (HFS : the abundances determined by adopting the HFS data taken from Kurucz 2001). The full table is available in electronic form at the CDS.

Ion	λ (Å)	χ (eV)	log gf	Ref.	log ϵ	Remark
He I	(log ϵ(He I) ≤9.0)		upper limit			
	5875.6				≤9.0	
	5875.60	20.96	−1.52	NI		
	5875.61	20.96	−0.34	NI		
	...	...	...	..		
	...	...	...	..		
	...	...	...	..		

For lines of C II λ 4267 Å, O I λ 6156–6158 Å, and Mg II λ 4481 Å, we used the line profile-fitting technique developed by Takeda (1995). All of these lines contain multiple line components so that the line profile-fitting technique is needed to reproduce the observed profiles.

We tried to adopt the most up-to-date and reliable transition probability data (log gf) whenever possible. We preferred to use oscillator strengths from the home page of NIST Atomic Spectra Database at the National Institute of Standards and Technology (NIST 2000). When new experimental data have been published after the NIST compilations, the NIST data were replaced with the new ones. The log gf values of several elements were taken from a number of references. These are as follows; C II – Hirata & Horaguchi (1995), V II – Biémont et al. (1989), Fe II – Raasen & Uylings (2000), La II – Lawler et al. (2001a), Ce II, Pr III, Nd III, and Dy III – DREAM web database of Biémont et al. (2002), Eu II – Lawler et al. (2001b), and Eu III – Mashonkina et al. (2002). When no data could be found in the literature, we used Kurucz (2001)'s data. References of the log gf values for individual lines are given in Table 2.

We used the damping constants in the VALD atomic line database (Kupka et al. 1999) for all the lines.

In analyses of Mn II, Co I and Eu II lines, effects of the hyperfine structures (HFS) were taken into account. The HFS data were adopted from Kurucz (2001). Some strong lines of Co II and doubly ionized lines of rare earth elements are known to be affected by HFS. Although such strong lines are used in the abundance estimation, we neglect the HFS effect because no data on HFS and IS (isotopic shift) are available.

The differences in abundances with and without HFS effect are negligibly small for Co I lines and Eu II lines, which are found to be −0.02 dex and −0.04 dex, respectively. However, large differences are found for Mn II lines (+0.21 dex). It is expected that the Zeeman pattern changes for some transitions in the presence of magnetic fields, and the HFS induces a perturbation of the pattern. Because HR 5049 has shown a very strong magnetic field of 4.7 kG, HFS only induces moderate perturbation of the pattern.

Table 3. Elemental abundances in HR 5049. Consecutive columns are as follows: the name of ion, the number of used lines, the derived abundance, the standard deviation, the solar log ϵ, and the logarithmic abundance for HR 5049 relative to the Sun.

Ions	n	log ϵ	S.D.	log $\epsilon\odot$	Δlog ϵ
He I		≤9.0		10.99	≤−2.0
C II		≤8.3		8.55	≤−0.25
O I		8.31		8.87	−0.56
Mg I	2	7.30	0.42	7.84	−0.54
Mg II	4	7.15	0.19		−0.69
Si II	3	7.75	0.09	7.55	+0.20
Cl II	3	7.39	0.17	5.5	+1.9
Sc II	1	3.06		3.17	−0.11
Ti II	6	5.49	0.38	5.02	+0.47
V II	1	4.75		4.00	+0.75
Cr I	4	7.61	0.45	5.67	+1.94
Cr II	18	7.36	0.48		+1.69
Mn II	3	6.30	0.00	5.39	+0.91
Fe I	10	8.32	0.17	7.50	+0.82
Fe II	35	8.29	0.32		+0.79
Co I	7	8.43	0.08	4.92	+3.51
Co II	12	8.35	0.37		+3.43
Ni II	1	6.90		6.25	+0.65
Sr II	2	2.96	0.16	2.97	−0.01
Y II	4	4.33	0.37	2.24	+2.09
Ba II	1	≤2.1		2.13	≤0.0
La II	1	4.00		1.17	+2.83
Ce II	4	4.68	0.21	1.58	+3.10
Pr II	1	4.70		0.71	+3.99
Pr III	10	4.68	0.27		+3.97
Nd III	3	4.74	0.13	1.50	+3.24
Eu II	2	4.06	0.42	0.51	+3.55
Eu III	2	5.30	0.42	0.51	+4.79
Gd II	5	4.53	0.28	1.12	+3.41
Dy II	1	4.75		1.14	+3.61
Dy III	1	4.07		1.14	+2.93

4. Results

We derived abundances of 28 ions for 21 elements and upper limits for three elements in HR 5049. Resultant abundances of individual lines are given in Table 2.

In Table 3, we summarize the averaged abundances. The mean abundances for each ion were calculated giving equal weight to all the lines. The columns in Table 3 from left to right are: the name of ion, the number of used lines, the derived abundance (log ϵ), the standard deviation, the solar log ϵ, and the logarithmic abundance relative to the Sun (Δlog ϵ). The solar abundances were taken from Grevesse et al. (1996).

4.1. Light elements

One of the striking findings in the spectrum of HR 5049 is the extreme weakness of neutral helium lines. As mentioned in Sect. 3, we found an extremely low abundance by ≤−2.0 dex (Fig. 1). Another strong He I line at λ 4471 Å is heavily contaminated. He I lines at λ 4120 Å, 4713 Å, and 4921 Å are absent. The weak line at λ 6678.15 Å gives the abundance with an upper limit of −1.0 dex. However, we prefer to adopt the result (−2.0 dex) obtained from the stronger line at λ 5875.6 Å.

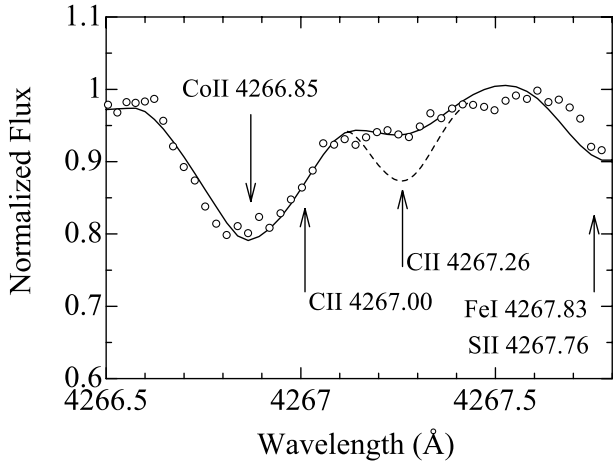

Fig. 3. The synthetic line profile fitting of the C II lines at λ 4267 Å. Open circles – the observed spectrum, dashed line – the solar abundance, and solid line – −0.25 dex compared with the solar value (adopted).

In Hg-Mn stars and Si stars, He lines are often quite weak. For some Hg-Mn stars, the following He abundances were obtained; −1.42 dex, −1.25 dex, and −1.7 dex for 112 Her A (=HD 174 933, Ryabchikova et al. 1996), κ Cnc (=HD 78 316, Adelman 1987), and 46 Aql (=HD 186 122, Sadakane et al. 2001), respectively. Ryabchikova & Stateva (1996) showed that the apparent He abundance varies from −0.59 dex to −1.29 dex in the He-weak star 36 Lyn (HD 79158). In their recent analysis of HR 1094, Nielsen & Wahlgren (2000) reported a He under-abundance of −0.89 dex. Quiet recently, Kochukhov et al. (2002) found a −3.0 dex He under-abundance in the CP2 star α^2 CVn (=HD 112 413, $T_{\rm eff}$ = 11 600 K, and log g = 4.02).

The He deficiency in HR 5049 is comparable with that in α^2 CVn. From the comparison with these recent abundance studies of chemically peculiar stars, we conclude that HR 5049 is an extremely He deficient CP star.

Figure 3 compares the observed spectrum with the synthetic one for the C II line at λ 4267 Å. The best fit is achieved for the case of −0.25 dex compared with the solar value. Since a Zr II line and a Ce II line exist near the C II 4267.26 Å line, the derived abundance for the C II lines should be taken as an upper limit.

The abundance of O determined from the O I λ 6156–6158 Å triplet lines (Fig. 4) shows a depletion by −0.56 dex. The oxygen abundance of HR 5049 agrees with those of other magnetic Ap stars (Takeda et al. 1999). Recent studies on NLTE line formation for O I lines suggest that the NLTE correction is limited within 0.2 dex (Takeda et al. 1999; Przybilla et al. 2000)

The abundance of Mg, derived from two Mg I lines and four Mg II lines including the λ 4481 Å line, suggests that Mg is slightly under-abundant in HR 5049. In HR 1094, a definite under-abundance of Mg was obtained by Nielsen & Wahlgren (2000).

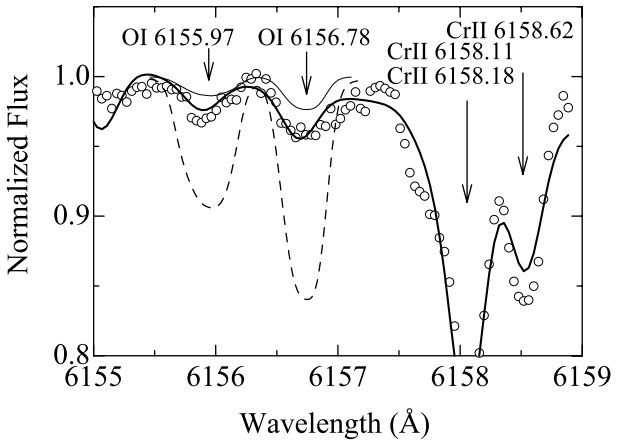

Fig. 4. The synthetic line profile fittings for the O I λ 6156–6158 Å triplet lines. Open circles – the observed spectrum, dashed line – the solar abundance, solid line – the adopted abundance (−0.56 dex), and thin solid line – −1.0 dex compared with the solar value.

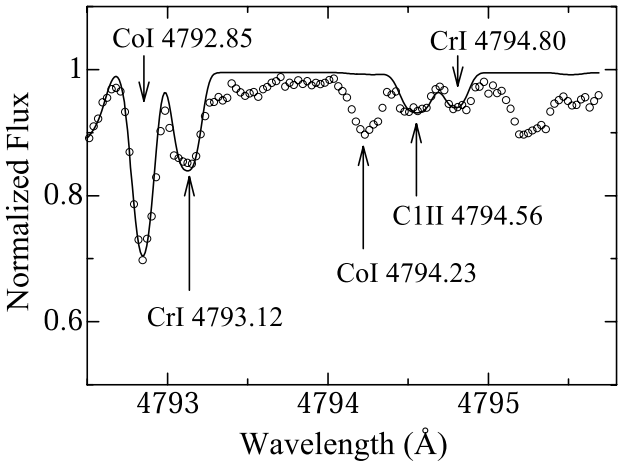

Fig. 5. The synthetic spectrum of the Cl II lines at λ 4794.56 Å. Open circles represent the observed spectrum, and solid line indicates the profile for the adopted abundance (7.21).

A slight over-abundance of Si in HR 5049, +0.2 dex, is found from three Si II lines. This is in sharp contrast with the under-abundance of Si in HR 1094 (Nielsen & Wahlgren 2000).

Three Cl II lines have been used to obtain the chlorine abundance. Figure 5 compares the observed spectrum with the synthetic one around the Cl II line at λ 4794.56 Å. Two lines at λ 4810 Å and λ 4819 Å are heavily contaminated by unknown lines. The Cl abundance of 7.4 is over-abundant by +1.9 dex comparing with the solar value. In a recent work on α^2 CVn, Kochukhov et al. (2002) shows that the relative local abundance of Cl reaches to an over-abundance by +4.7 dex in its negative magnetic pole.

4.2. Iron peak elements

All of the iron peak elements, from Ti through Ni, are found to be over-abundant by more than +0.5 dex.

Iron shows a high abundance of 8.30, which is significantly higher than the solar value (7.50) and similar to that found in HR 1094 (8.45 and 8.46, Sadakane 1992 and Nielsen & Wahlgren 2000, respectively).

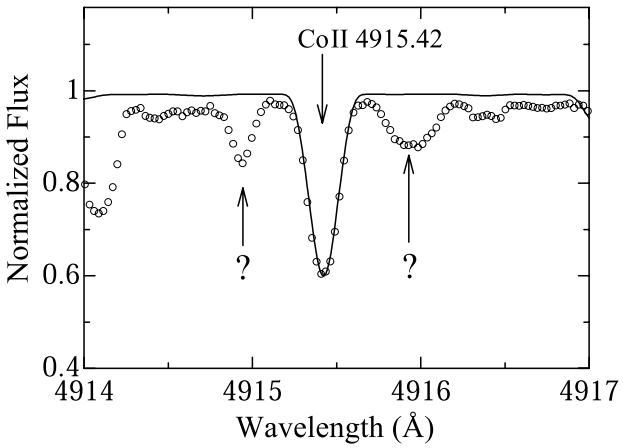

Fig. 6. The synthetic spectrum of the Co II lines at λ 4915.42 Å. Open circles represent the observed spectrum, and solid line indicates the profile for the adopted abundance (8.50). Unidentified features are indicated by question marks.

Another remarkable result is the large over-abundance of Co (+3.5 dex). Figure 6 shows an analysis of one of strong Co II line at λ 4915.42 Å. For HR 1094, Nielsen & Wahlgren (2000) reported an over-abundance by +3.0 dex, confirming the earlier result of Sadakane (1992). In an abundance analysis of the roAp star HD 166 473, Gelbmann et al. (2000) showed an over-abundance by +1.09 dex. Abundances of Ca, Ti, Fe, and Ni in HD 166 473 are close to the solar values, while Cr and Mn are over-abundant. Recently, Cowley et al. (2000) derived an over-abundance of Co by +1.6 dex in Przybylski's star (HD 101 065). These studies suggest that the over-abundance of Co found in HR 5049 is one of the most extreme among CP stars.

4.3. Heavy and rare earth elements

Among heavy elements including rare earth elements, Ba is an exception. The Ba II line at λ 4554 Å is very weak (Fig. 7). The upper limit of Ba abundance is nearly the solar value. It is interesting to find a low abundance of Ba in view of the large over-abundances (more than 3 dex) of neighboring rare earth elements such as La and Ce.

All of the rare earth elements in HR 5049 are over-abundant by more than +2.8 dex compared with the solar values.

The abundance of La has been derived from only one La II line. La has one stable isotope and shows HFS. The HFS does not influence the final abundance because of the weakness of the line. No La III lines listed in Biémont et al. (2002) was detected.

Many clean Ce II lines are seen in the spectrum. We can determine the magnetic intensifications due to the Zeeman effect for four lines, from which we derive an over-abundance of Ce by +3.10 dex. According to Aoki et al. (2001), the hyperfine splitting of Ce II is zero. No line of Ce III listed in Bord et al. (1997) could be found.

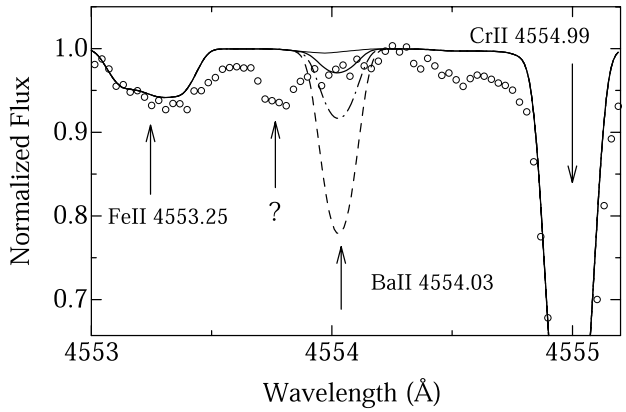

Fig. 7. The synthetic spectrum of the Ba II line at λ 4554.03 Å. Open circles – the observed spectrum, dashed line – +1.0 dex, dot-dashed line – +0.5 dex, solid line – solar abundance (adopted), and thin solid line – −1.0 dex compared with the solar value. An unidentified feature is indicated by a question mark.

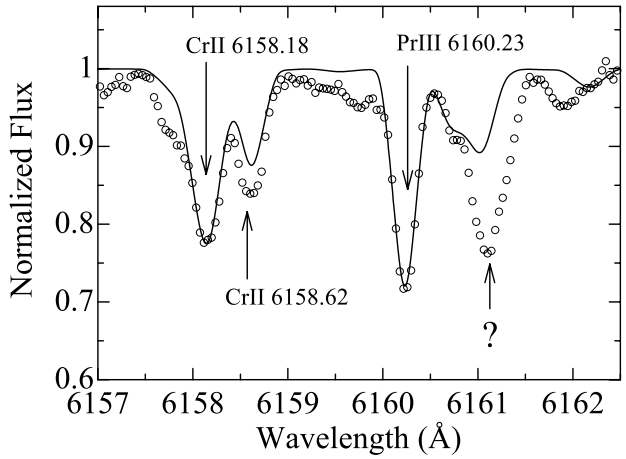

Fig. 8. The synthetic spectrum of the Pr III line at λ 6160.23 Å. Open circles represent the observed spectrum, and the solid line indicates the profile for the adopted abundance. An unidentified feature is indicated by a question mark.

For Pr, one weak Pr II line and 12 strong Pr III are used in the abundance determination to find an over-abundance of +3.97 dex. Although Dolk et al. (2002) stated some Pr III lines show asymmetric profiles, no line shows such a profile in the spectrum of HR 5049. Figure 8 shows an analysis of one of the strong Pr III lines at λ 6160.23 Å .

The abundance of Nd (+3.24 dex over-abundant) was deduced from three Nd III lines. As noted in Dolk et al. (2002), Nd has seven stable isotopes, but the isotopic effects are known to be not serious.

Eu is found to be over-abundant by +3.6 dex, from the analyses of two Eu II lines. The hyperfine splitting is included in our calculations. The abundance derived from the Eu III lines is fairly larger than that derived from Eu II lines. The Eu III λ 6666.35 Å line gives an Eu abundance of 5.00, though this line is contaminated by Cr II and Fe II lines. Mashonkina et al. (2002) calculated NLTE effects on both the Eu II λ 6645.11 Å line and the Eu III λ 6666.35 Å line for α^2 CVn ($T_{\rm eff}$ = 11 500 K, log g = 4.0). They showed that NLTE corrections in this star are +0.43 and −0.10 for the former and the latter lines, respectively. When we apply their NLTE corrections to these two lines in HR 5049, the difference of abundances deduced from these two lines decreases from 1.13 dex to 0.60 dex.

Table 4. Abundance changes for each ion in HR 5049. ΔM: the abundance difference due to the change of the metallicity from [M/H] = 1.0 to 0.0. $\Delta T+$: $T_{\rm eff}$ = 10 300 K + 300 K (increase $T_{\rm eff}$ by 300 K), $\Delta T-$: $T_{\rm eff}$ = 10 300 K − 300 K, $\Delta G+$: log g = 3.81 + 0.2, and $\Delta G-$: log g = 3.81 − 0.2.

Ion	ΔM	$\Delta T+$	$\Delta T-$	$\Delta G+$	$\Delta G-$
C II	+0.20	−0.05	−0.05	+0.05	−0.10
O I	+0.05	+0.04	0.00	0.00	0.00
Mg I	−0.14	+0.17	−0.17	−0.07	+0.07
Mg II	−0.05	−0.14	−0.08	0.00	−0.05
Si II	+0.11	−0.04	+0.04	+0.03	−0.02
Cl II	+0.27	−0.14	+0.15	+0.11	−0.11
Sc II	−0.14	+0.18	−0.18	0.00	+0.01
Ti II	−0.10	+0.15	−0.12	+0.03	−0.01
V II	−0.10	+0.09	−0.09	+0.04	−0.03
Cr I	−0.14	+0.20	−0.20	−0.06	+0.07
Cr II	+0.03	+0.03	−0.02	+0.05	−0.03
Mn II	−0.04	+0.03	−0.03	+0.04	−0.04
Fe I	−0.14	+0.16	−0.16	−0.06	+0.05
Fe II	+0.04	+0.02	−0.02	+0.06	−0.05
Co I	−0.12	+0.15	−0.15	−0.05	+0.06
Co II	+0.07	−0.01	−0.01	+0.05	−0.06
Ni II	+0.20	−0.08	+0.07	+0.06	−0.07
Sr II	−0.14	+0.18	−0.18	−0.04	+0.04
Y II	−0.15	+0.22	−0.22	−0.03	+0.03
Ba II	−0.16	+0.21	−0.23	−0.04	+0.04
La II	−0.15	+0.24	−0.25	−0.04	+0.04
Ce II	−0.17	+0.21	−0.22	−0.03	+0.03
Pr II	−0.15	+0.24	−0.24	−0.04	+0.05
Pr III	+0.01	+0.05	−0.08	+0.04	−0.06
Nd III	+0.01	+0.05	−0.08	+0.04	−0.06
Eu II	−0.13	+0.21	+0.01	+0.09	−0.09
Eu III	0.00	−0.02	−0.24	−0.04	+0.03
Gd II	−0.15	+0.21	−0.20	−0.02	+0.03
Dy II	−0.16	+0.22	−0.22	−0.04	+0.04
Dy III	−0.04	+0.03	−0.03	+0.08	−0.08

4.4. Errors in the abundance analysis

In Table 4, we present the expected difference in the abundances due to the change of the model atmospheric parameters.

ΔM: the abundance difference due to the change of the metallicity from [M/H] = 1.0 to 0.0. The abundances derived from the two models for each ion show the discrepancy within 0.2 dex except for Cl;

$\Delta T+$ and $\Delta T-$: the abundance difference due to the change of the effective temperature by +300 K ($\Delta T+$) and −300 K ($\Delta T-$). We find the changes within 0.24 dex;

$\Delta G+$ and $\Delta G-$: the abundance difference introduced by changing the surface gravity by + 0.2 ($\Delta G+$) and − 0.2 ($\Delta G-$). We find a small difference within 0.11 dex.

Table 5. Comparison of elemental abundances in HR 5049 with three CP2 stars.

Ions ($T_{\rm eff}$, log g)	HR 5049[1] (10 300 K, 3.81)	HR 1094[2] (12 000 K, 4.2)	HD 187 474[5] (10 400 K, 4.0)	HD 166 473[6] (7700 K, 4.20)
He I	≤9.0	10.1		
C II	≤8.3			
O I	8.31	8.1	8.17	7.33
Mg I	7.30			7.01
Mg II	7.15	6.6		7.73
Si II	7.75	6.8	7.70	8.07
Cl II	7.39	8.1		
Sc II	3.06	≤3.4	3.17	4.13
Ti II	5.49	6.69	5.02	4.97
V II	4.75		4.00	5.17
Cr I	7.61			6.50
Cr II	7.36	7.02	7.82	6.64
Mn II	6.30		7.17	6.70
Fe I	8.32			7.66
Fe II	8.29	8.46	8.39	7.69
Co I	8.43			5.97
Co II	8.35	7.92		
Ni II	6.90	≤5.8		
Sr II	2.96	4.32[3]		5.00
Y II	4.33			4.14
Ba II	≤2.1	≤3.1		1.63
La II	4.00			3.70
Ce II	4.68	5.2		4.45
Pr II	4.70			3.19
Pr III	4.68		4.55	4.40
Nd III	4.74		4.44	5.57
Eu II	4.06	3.8		3.57
Eu III	5.30			
Gd II	4.53		4.13	
Dy II	4.75	4.6, 6.2[4]		4.21
Dy III	4.07			

[1] This work.
[2] Nielsen & Wahlgren (2000).
[3] Sadakane (1992).
[4] Values derived at two different epochs.
[5] Strasser et al. (2001).
[6] Gelbmann et al. (2000).

5. Discussion

A spectrum synthesis analysis for 24 chemical elements has been carried out for the magnetic B star HR 5049 in this study.

In Fig. 9, we compare the elemental abundances obtained in HR 5049 with those in the Sun.

In Table 5, we compare the chemical abundances of HR 5049 with those found in recent works on some CP2 stars. The first column in Table 5 is the name of ion, the second is the elemental abundances of HR 5049 (this work), and the third is those of HR 1094 which are taken from Nielsen & Wahlgren (2000) and Sadakane (1992). The fourth column is the abundances in HD 187 474 (HR 7552, Strasser et al. 2001), for which their best fitting uniform abundances are given in Table 5. The final column is the abundances of the roAp star HD 166 473 (Gelbmann et al. 2000).

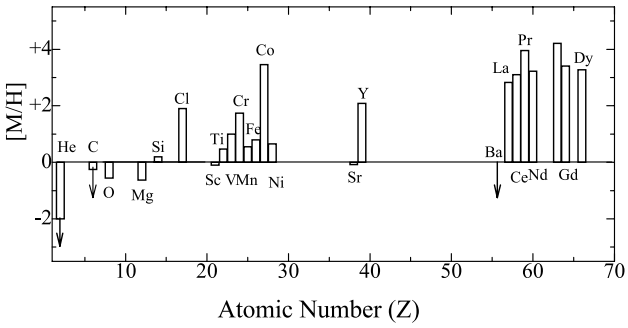

Fig. 9. The abundances in logarithmic units for HR 5049 compared with the solar values. Upper limits for three elements are shown by downward arrows.

In HR 5049, most of the light elements (He, C, O, Mg) are under-abundant. Especially, the under-abundance of He by

−2.0 dex is highly conspicuous. Si shows the solar abundance, while Cl is over-abundant by +1.9 dex. Most of the iron peak elements are over-abundant by more than 0.5 dex with respect to the solar values.

Although the abundance pattern of iron peak elements in HR 5049 is almost within the range of those in other CP2 stars, the over-abundance of Co is remarkable. The derived abundance of Co in this study is highest among the stars reported so far.

Abundances of observed rare earth elements exhibit the excess by more than +3.0 dex compared with the solar abundances. Among others, Pr and Eu show very large over-abundance by +4 dex.

We find uncomfortably large standard deviations in the derived abundances of some ions such as Ti II, Cr II and Co II, and also large discrepancies of Mg and Cr abundances obtained from the neutral and singly ionized lines. We think these discrepancies might be (partly) understood when we introduce the vertical stratifications of the elements in question in the atmospheric layer of HR 5049. For example, the weak Cr II lines (equivalent width smaller than 50 mÅ) or high excitation Cr II lines (5 eV or higher) yield a high abundance of 8.0 dex, while strong lines yield a low abundances of 7.0 dex. The same tendency is found for Fe II lines; a high abundance of 8.5 dex is obtained from weak lines (equivalent width smaller than 100 mÅ), while a low abundance of 7.7 dex is obtained from strong lines. These discrepancies are too large to be explained in term of errors in the model atmosphere or observational errors. Recently, Ryabchikova et al. (2002) examined the abundance stratification in the roAp star γ Equ (HD 201 601). They showed that Ca, Cr, Fe, Ba, Si, and Na seem to be over-abundant in deeper layers, but normal or even under-abundant in the upper layers, which are the same tendencies found for Cr and Fe in HR 5049.

Finally, we briefly discuss the relation between the Nd and Pr abundances found among CP stars. For cool Hg-Mn stars and Am stars, Dolk et al. (2002) have reported the presence of an apparent dependence of the abundance difference between Nd and Pr on the effective temperature.

In Fig. 10, we plot the Nd-Pr abundance difference against the $T_{\rm eff}$ for various CP stars including HR 5049. The difference is smaller than 0.8 dex (the solar value of log (Nd/Pr)) for hotter ($T_{\rm eff} \geq 10\,000$ K, Hg-Mn group) stars. On the other hand, we find larger differences (1.0 dex or more) in cooler magnetic stars. Although these abundances in CP stars were determined by different authors at single phases in most cases, and they should not represent averaged abundances over the stellar surfaces, the upper envelope of the diagram of Nd-Pr abundance difference apparently decreases with the increasing $T_{\rm eff}$.

For HR 5049, the Nd-Pr abundance difference is 0.06 dex. This is quite small when compared with other CP stars. Another example with a similar Nd-Pr difference can be found in HD 187 474. Strasser et al. (2001) obtained surface abundance distributions for this very slowly rotating magnetic Ap star ($T_{\rm eff}$ = 10 400 K, log g = 4.0, the magnetic field of 5 to 6 kG). Its abundance pattern is similar to that found in HR 5049 (Table 5). The Nd-Pr abundance difference in HD 187 474 is −0.11 dex. Recently, Kato (2003) derived the Nd-Pr abundance difference of the weak magnetic silicon star HR 6958 (=HD 170 973, $T_{\rm eff}$ = 10 750 K, log g = 3.5) to be +0.24 dex. The Nd-Pr abundance differences of these stars, especially those in HR 5049 and HD 187 474, are quite small when compared to the Nd-Pr abundance differences of Hg-Mn stars obtained by Dolk et al. (2002). The surface temperatures of HR 5049, HD 187 474 and HR 6958 are just at the boundary ($T_{\rm eff}$ = 10 500 K) where Dolk et al. (2002) found an abrupt change in the the Pr and Nd abundances. The peculiar abundance pattern of Pr and Nd in these stars might be physically connected with the disappearance or diminishing of the H convection zone at $T_{\rm eff}$ = 10 500 K (Dolk et al. 2002).

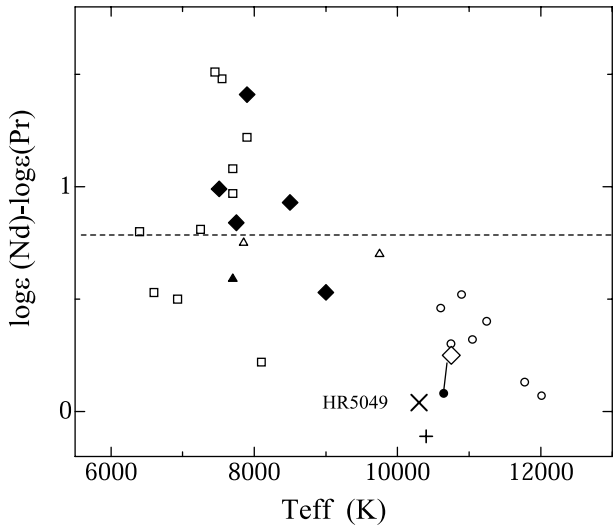

Fig. 10. The relation between the Nd-Pr abundance differences and the effective temperature of various CP stars. Small open circles (Hg-Mn stars) and small open triangles (Am stars) are taken from Dolk et al. (2002). The small filled circle (HR 7775, Hg-Mn star) and the small filled triangle (Am star) are taken from Ryabchikova et al. (2001). The small open circle connecting with the small filled circle is for HR 7775, which are taken from Dolk et al. (2002). Small open squares (roAp stars) are taken from Ryabchikova et al. (2001), Cowley et al. (2000), Kochukhov (2003), Gelbmann et al. (2000), and Ryabchikova et al. (2000). Filled diamonds (non-pulsating CP2 stars) are taken from Ryabchikova et al. (2001). The plus sign (HD 187 474, CP2 star) and the open diamond (HR 6958 = HD 170 973, Si star) are taken from Strasser et al. (2001) and Kato (2003), respectively. The St. Andrew's cross is for HR 5049 (this study). All the log gf values of these authors are transformed into our scale. The horizontal broken line indicates the solar value.

It seems to be interesting to extend the study of the abundance differences to other pairs of elements such as Ce-Pr and Sm-Eu in various CP stars. Then it may become possible to make a detailed diagnosis concerning the complex physical interplay between the atomic structure and the atmospheric processes such as diffusion, convection, magnetic field, and mass loss in CP stars.

Acknowledgements. We deeply thank Drs. E. Biémont and P. Quinet for kindly providing us information on atomic data. We also thank Dr. A. Wahlgren for his helpful comments and suggestions which enabled us to improve the original manuscript.

References

Adelman, S. J. 1987, MNRAS, 228, 573
Adelman, S. J., Gulliver, A. F., & Lodén, L. O. 2000, A&A, 353, 335
Aoki, W., Ryan, S. G., Norris, J. E., et al. 2001, ApJ, 561, 346
Biémont, E., Grevesse, N., Faires, L. M., et al. 1989, A&A, 209, 398
Biémont, E., Palmeri, P., & Quinet, P. 2002, http://www.umh.ac.be/~astro/dream.shtml
Bord, D. J., Cowley, C. R., & Norquist, P. L. 1997, MNRAS, 284, 869
Castelli, F., & Kurucz, R. L. 1994, A&A, 281, 817
Castelli, F., Parthasarathy, M., & Hack, M. 1997, A&A, 321, 254
Cowley, C. R., & Aikman, G. C. L. 1980, ApJ, 242, 684
Cowley, C. R., Ryabchikova, T., Kupka, F., et al. 2000, MNRAS, 317, 299
Dolk, L., Wahlgren, G. M., Lundgerg, H., et al. 2002, A&A, 385, 111
Dworetsky, M. M. 1982, Observatory, 102, 138
Dworetsky, M. M., Trueman, M. R. G., & Stickland, D. J. 1980, A&A, 85, 138
Gelbmann, M., Ryabchikoba, T., Weiss, W. W., et al. 2000, A&A, 356, 200
Grevesse, N., Noels, A., & Sauval, A. J. 1996, in Cosmic Abundances, ed. S. S. Holt, & G. Sonneborn (San Francisco: ASP), PASPC, 99, 117
Hensberge, H. 1993, in Peculiar Versus Normal Phenomena in A-Type and Related Stars, IAU Coll. 138, ed. M. M. Dworetsky, F. Castelli, & R. Faraggiana (San Francisco: ASP), PASPC, 44, 547
Hirata, R., & Horaguchi, T. 1995, http://vizier.u-strasbg.fr/cgi-bin/VizieR?-source=VI/69
Hubrig, S., North, P., & Mathys, G. 2000, ApJ, 539, 352
Kato, K. 2003, PASJ, 55, 1133
Kochukhov, O. 2003, A&A, 404, 669
Kochukhov, O., Piskunov, N., Ilyin, I., Ilyina, S., & Tuominem, I. 2002, A&A, 389, 420
Kupka, F., Piskunov, N., Ryabchikova, T. A., Stempels, H. C., & Weiss, W. W. 1999, A&AS, 138, 119
Kurucz, R. L. 1993, ATLAS9 Stellar Atmosphere Programs and 2km/s Grid, Kurucz CD–ROM No.13, Smithsonian Astrophysical Observatory, Cambridge, MA
Kurucz, R. L. 1996, in M.A.S.S. Model Atmospheres and Spectrum Synthesis, ed. S. J. Adelman, F. Kupka, & W. W. Weiss (San Francisco: ASP), PASPC, 108, 160
Kurucz, R. L. 2001, http://kurucz.harvard.edu/
Kurucz, R. L., & Bell, B. 1995, Atomic Data for Opacity Calculations, Kurucz CD–ROM No.23, Smithsonian Astrophysical Observatory, Cambridge, MA
Landstreet, J. D., & Mathys, G. 2000, A&A, 359, 213
Lawler, J. E., Bonvallet, G., & Sneden, C. 2001a, ApJ, 556, 452
Lawler, J. E., Wickliffe, M. E., & Den Hartog, E. A. 2001b, ApJ, 563, 1075
Lester, J. B., Gray, R. O., & Kurucz, R. L. 1986, ApJS, 61, 509
Mashonkina, L. I., Ryabtsev, A. N., & Ryabchikova, T. A. 2002, Astro. Lett., 28, 34
Mathys, G. 1990, A&A, 232, 151
Mathys, G., & Hubrig, S. 1997, A&AS, 124, 475
Mathys, G., & Hubrig, S. 2004, in preparation
Mathys, G., Hubrig, S., Landstreet, J. D., Lanz, T., & Manfroid, J. 1997, A&AS, 123, 353
Moon, T. T., & Dworetsky, M. M. 1985, MNRAS, 217, 305
Moore, C. E., Minnaert, M. G. J., & Houtgast, J. 1966, The Solar Spectrum 2935 Å to 8770 Å, NBS Monograph 61 (Washington, DC: US Government Printing Office)
Nielsen, K., & Wahlgren, G. M. 2000, A&A, 356, 146
Nishimura, M. 1998, PASJ, 50, 285 (Paper I)
NIST 2000, http://physics.nist.gov/PhysRefData/contents-atomic.html
North, P., & Nicolet, B. 1994, A&A, 286, 348
Przybilla, N., Butler, K., Becker, S. R., Kudritzki, R. P., & Venn, K. A. 2000, A&A, 359, 1085
Raasen, A. J. J., & Uylings, P. H. M. 2000, http://www.science.uva.nl/pub/orth/iron/FeII.E1
Ryabchikova, T. A., & Stateva, I. 1996, in M.A.S.S. Model Atmospheres and Spectrum Synthesis, ed. S. J. Adelman, F. Kupka, & W. W. Weiss (San Francisco: ASP), PASPC, 108, 265
Ryabchikova, T. A., Zakharova, L. A., & Adelman, S. J. 1996, MNRAS, 283, 1115
Ryabchikova, T. A., Savanov, I. S., Hatzes, A. P., Weiss, W. W., & Handler, G. 2000, A&A, 357, 981
Ryabchikova, T. A., Savanov, I. S., Malanushenko, V. P., & Kudryavtsev, D. O. 2001, Astron. Rep., 45, 382
Ryabchikova, T. A., Piskunov, N., Kochukhov, O., et al. 2002, A&A, 384, 553
Sadakane, K. 1992, PASJ, 44, 125
Sadakane, K., Takada-Hidai, M., Takeda, Y., et al. 2001, PASJ, 53, 1223
Strasser, S., Landstreet, J. D., & Mathys, G. 2001, A&A, 378, 153
Takeda, Y. 1993, PASJ, 45, 453
Takeda, Y. 1995, PASJ, 47, 287
Takeda, Y. 2000, private communication
Takeda, Y., Takada-Hidai, M., Jugaku, J., Sakaue, A., & Sadakane, K. 1999, PASJ, 51, 961